

1 **droplet-Tn-Seq combines microfluidics with Tn-Seq identifying complex single-cell phenotypes**

2

3

4 Derek Thibault¹, Stephen Wood¹, Paul Jensen^{1,2} and Tim van Opijnen^{1,*}

5

6

7 ¹Biology Department, Boston College, Chestnut Hill, MA, USA

8

9

10 ² Present address:

11 Department of Bioengineering and Carl R. Woese Institute for Genomic Biology, University of Illinois
12 at Urbana-Champaign, Urbana, IL, USA

13

14

15

16

17

18

19 * Corresponding Author

20

21

22

23 **Abstract**

24 While Tn-Seq is a powerful tool to determine genome-wide bacterial fitness in high-throughput,
25 culturing transposon-mutant libraries in pools can mask community or other complex single-cell
26 phenotypes. droplet-Tn-seq solves that problem by microfluidics facilitated encapsulation of individual
27 transposon mutants into liquid-in-oil droplets, thereby enabling isolated growth, free from the influence
28 of the population. Importantly, all advantages of Tn-Seq are conserved, while reducing costs and greatly
29 extending its applicability.

30

31 **Main text**

32 Transposon insertion sequencing (Tn-Seq) has become the gold standard to determine in high-
33 throughput and genome-wide a gene's quantitative contribution to fitness under a specific growth
34 condition (van Opijnen et al. 2009). It has been successfully applied to bacteria, yeast and eukaryotes
35 and has enabled the discovery of new biology including gene function, non-coding RNAs and host-
36 factors affecting disease susceptibility (van Opijnen & Camilli 2013). One of the biggest strengths of
37 Tn-Seq is the ability to screen hundreds of thousands of mutants in a single experiment. However,
38 growing mutants *en masse*, i.e. in a pool, can mask the fitness of certain mutants. For instance, secreted
39 factors that break down complex glycans into smaller units for energy utilization, can be viewed as
40 community factors since mutants that do not produce these enzymes can 'cheat' and reap the carbon-
41 source benefits. Moreover, additional mechanisms including frequency dependent selection, bet-hedging
42 and division of labor can retain mutants with a relatively low individual fitness in a population, which
43 are all missed by Tn-Seq (Veening et al. 2008; Sæther & Engen 2015).

44

45 In order to obtain a comprehensive understanding of a complex population it is thus important to
46 consider the fitness of each individual in isolation as well as in the context of the population. To achieve
47 this we developed droplet-Tn-Seq (dTn-Seq), by combining Tn-Seq with microfluidics. In dTn-Seq a
48 microfluidic device enables encapsulation of millions of single bacterial cells in micron-sized droplets in
49 which bacteria are cultured. Each transposon mutant thus starts off in a complex pool of mutants, is then
50 separated and cultured in isolation, and finally cells are pooled back together. Before encapsulation and
51 after pooling, genomic DNA is isolated for sample preparation and the change in frequency of each
52 mutant over the course of the experiment is determined through massively parallel sequencing, which is
53 used to calculate individual growth rates (van Opijnen et al. 2009). Therefore, through strategic isolation
54 and pooling, dTn-Seq enables the establishment of single cell behavior in a genome-wide and high-
55 throughput fashion (Fig. 1a). Moreover, we show that besides the ability to resolve complex single-cell
56 behavior, droplets have many more advantages and applications including a drastic reduction in culture
57 media volume (and possible expensive compounds), and analyses of interactions between bacteria
58 and/or host-cells.

59

60 To enable encapsulation of single cells into a single droplet, microfluidic devices were designed and
61 built in-house (Fig. 1b, Supplementary File 1), which depending on oil and aqueous phase flow rates
62 generate droplets with a diameter of $\sim 67 \mu\text{M}$ at a rate of $\sim 5 \times 10^4$ droplets/minute. Droplets are composed
63 of an outer oil-surfactant layer and are filled with growth media ($\sim 157\text{pL}$; Fig. 1c, d). They enable

64 robust bacterial growth for Gram-negative and positive bacteria alike and support overall growth
65 dynamics comparable to bacteria grown in batch culture (a large e.g. 5ml culture; Fig. 1e). Pooled
66 transposon libraries, where each bacterial cell contains a single transposon insertion, are separated as
67 single cells by encapsulation and cultured inside the droplet for 5-8 generations. With (d)Tn-Seq,
68 massively parallel sequencing is used to determine the exact location of a transposon insertion and by
69 sequencing two time points (i.e. at the start and end of the experiment) the frequency of each mutant can
70 be accurately quantified which is used to calculate the transposon's impact on the growth rate (van
71 Opijnen et al. 2009, van Opijnen & Camilli 2013). Due to the small volume of the droplet the amount of
72 genomic DNA obtained from a dTn-Seq experiment is not sufficient for sample preparation. To
73 overcome this a whole genome amplification (WGA) step, mediated by phi29 is introduced. WGA
74 conditions were optimized so that when dTn-Seq library preparation is compared against the standard
75 Tn-Seq approach no bias is observed ($R^2=0.89$; Fig. 1f) and reproducibility is very high ($R^2=0.88$; Fig.
76 1g).

77

78 To determine the functionality of dTn-Seq, transposon insertion libraries of *Streptococcus pneumoniae*
79 were grown in batch-culture as a pooled population ('standard' Tn-Seq) and encapsulated as single cells
80 (dTn-Seq) in growth media with either glucose or the complex glycan alpha-1-acid glycoprotein (AGP)
81 as the major carbon source. Moreover, by adding low-melting temperature agarose to growth media with
82 glucose, droplets with a 1% agarose density were generated to assess how a solid environment that
83 provides structural support affects single cell growth. For each gene in each condition, fitness (i.e. the
84 growth rate) was calculated and compared between pooled-batch and droplet conditions. Overall, 2-5%
85 of genes from a variety of categories, including metabolism, transport, regulation and cell wall integrity
86 have a significantly different fitness (Supplementary Fig. 1), indicating that population structure, i.e. the
87 droplet environment, can significantly affect clonal fitness.

88

89 To validate dTn-Seq a total of 7 genes were chosen from the three environments (Supplementary Fig. 1;
90 Supplementary Tables 1-5). In the simplest environment with glucose as the carbon source $\Delta lytB$
91 (SPT_1238) has no effect on fitness, however when grown in droplets the mutant has a severe growth
92 defect (Fig. 2a, b; Supplementary Fig. 1; Supplementary Table 1). This defect seems to be due to the
93 small droplet environment, since poor growth is masked when the mutant is grown by itself in batch
94 culture (5ml; Fig. 2b). LytB is part of the lytic cycle of *S. pneumoniae* and is involved in cell-chain
95 shortening (García et al. 1999). Indeed, chain-length of $\Delta lytB$ is significantly longer than the wt when
96 grown in batch, however when the mutant is grown in droplets, chain-lengths are shortened and

97 indistinguishable from wt (Fig. 2a). Recently longer cell chains were associated with rapid local
98 induction of competence (Domenech et al. 2018), which we hypothesized could be further enhanced in
99 the micro-droplet environment. Gene-expression of a set of competence genes was compared between
100 wt and Δ *lytB* grown in batch and in droplets. As posited, competence genes of Δ *lytB* cultured in droplets
101 are highly upregulated (Fig. 2c). Importantly, competence also induces the autolysin *cbpD* as well as the
102 immunity gene *comM*. In Δ *lytB*-droplets *comM* is upregulated ~8-fold, while *cbpD* is upregulated ~28-
103 fold. This means that, especially in a confined space, *LytB* is extremely important in limiting a local
104 hypercompetent phenotype, which when deleted triggers autolysis and fratricide and reduces fitness.

105

106 We next compared transposon libraries grown in culture medium with AGP as the major carbon source.
107 AGP is a highly glycosylated protein found in serum with covalently linked carbohydrate side chains
108 composed of linked monosaccharides such as mannose, galactose, N-acetylglucosamine (GlcNAc/GlcN),
109 and sialic acid. Most bacteria, including *S. pneumoniae*, are unable to take up such large structures and
110 depend on monosaccharides being liberated, for instance by secreted enzymes (King 2010). Four genes
111 (SP_1415/*nagB*, SP_1674, SP_1685/*nanE*, SP_2056/*nagA*) with a severe growth defect in AGP-droplets
112 and no defect in batch culture were validated. Each gene is dispensable when grown by itself in media
113 with glucose but is highly important for growth when AGP is the carbon source (Fig. 2d; Supplementary
114 Fig. 1; Supplementary Table 4). Importantly, when a deletion mutant of either gene is grown in the
115 presence of the wildtype the growth defect in AGP is masked (Fig. 2d), indicating that the wildtype is
116 providing community support and compensating the mutant's fitness. While none of the four genes have
117 previously been shown to be influenced by the community, each gene is associated with either
118 regulating, releasing and/or processing AGP-linked monosaccharides. Specifically, SP_1415/*nagB* and
119 SP_2056/*nagA* have been shown in other species to be involved in processing GlcN and GlcNAc (Moye
120 et al. 2014), SP_1674 is a predicted transcriptional activator of a regulon containing *nanA* and *nanB*
121 which have been show to release sialic acid from complex glycan structures (King 2010), and
122 SP_1685/*nanE* is a putative lipoprotein anchored to the membrane and important for sialic acid
123 utilization (Pélissier et al. 2014). These data show that dTn-Seq is highly sensitive in identifying genes
124 and processes that can be shared amongst bacteria and enable 'cheating', which are missed with Tn-Seq.

125

126 | Lastly, two capsule genes (SPT_0394/*cpsC*, SPT_0395/*cpsD*) were validated that are very important for
127 growth under standard conditions (e.g. liquid media), but whose fitness is largely compensated by the
128 addition of 1% agarose (Fig. 2f; Supplementary Fig. 1; Supplementary Table 2). Like liquid droplets,
129 agarose droplets are monodisperse and have a similar volume (Supplementary Fig. 2). Indeed, when the

130 deletion mutants are cultured in liquid droplets or in batch, SPT_0394 hardly grows, while SPT_0395
131 grows slower than the wt, reflecting their fitness (Fig. 2f). In contrast, the 1% agarose environment
132 allows both mutants to expand robustly, and form microcolonies similar to wt (Fig. 2f,g). Microcolony
133 formation is important for bacterial survival in host-tissue, and for instance makes *Pseudomonas*
134 *aeruginosa* less sensitive to antimicrobials (Lam et al. 1980; Worlitzsch et al. 2002; Sriramulu et al.
135 2005). Microcolonies and biofilms are both formed by clusters of bacteria and thus dTn-Seq could
136 provide a proxy to uncover genes that are important under such circumstances. Importantly, noncapsular
137 *S. pneumoniae* strains are often better at biofilm formation (Domenech et al. 2012), which is suggestive
138 for the improved performance of the capsule mutants in agarose.

139
140 To conclude, dTn-Seq is a valuable extension of Tn-Seq that is able to uncover novel single-cell
141 phenotypes associated with microenvironments, community factors, and solid environments that are
142 masked by Tn-Seq. dTn-Seq is applicable to practically any bacterium and any variation of Tn-Seq (e.g.
143 IN-Seq, TraDIS, HITS, Bar-Seq). Importantly, we have only shown a limited number of environments
144 but there are many other possibilities. For instance, we have successfully used dTn-Seq in combination
145 with antibiotics, in a screen for siderophores, and to determine interactions between bacteria and host-
146 cells. Moreover, agarose droplets are sortable via FACS and droplets are easily imaged. Lastly, the small
147 droplet environment reduces the amount of (expensive) compounds and chemicals needed to perform an
148 experiment (e.g. AGP) thereby enabling genome-wide studies for a fraction of the cost.

149 |

150 **Methods**

151

152 **Bacterial strains, growth and media.**

153 Sequencing and validation experiments were performed using *Streptococcus pneumoniae* TIGR4 (NCBI
154 Reference Sequence: NC_003028.3), and Taiwan-19F (NC_012469.1). Other species used in the study
155 were *Yersinia pestis* (KIM6, pCD1 negative and pgm negative), *Escherichia coli* (DH5- α),
156 *Acinetobacter baumannii* (ATCC 17978), *Staphylococcus aureus* (RN1, NR-45904), *Klebsiella*
157 *pneumoniae* (UHKPC57, NR-44357), *Pseudomonas aeruginosa* (PA14), *Enterobacter aerogenes*
158 (NRRL B-115), and *Enterobacter cloacae* (NRRL B-412). Except for specific growth and selection
159 experiments the *S. pneumoniae* strains were cultured statically in Todd Hewitt broth supplemented with
160 yeast extract (THY) plus 5 μ l/ml Oxyrase (Oxyrase, Inc.) and 150 U/ml catalase (Worthington Bio Corp
161 LS001896), or on Sheep's blood agar plates at 37°C in a 5% CO₂ atmosphere. *Y. pestis* was cultured in
162 brain heart infusion media or on blood agar while all other strains were cultured in Luria-Bertani (LB)
163 broth or on LB agar at 37°C. Unless otherwise noted cells were cultured to exponential phase before
164 being washed in PBS and diluted down into the appropriate media.

165

166 **Transposon library construction and selection experiments.**

167 Library construction using the mariner transposon Magellan6 was performed as previously described
168 (van Opijnen & Camilli 2013; van Opijnen & Camilli 2012; van Opijnen et al. 2009). The transposon
169 lacks transcriptional terminators allowing for read-through transcription, and additionally has stop
170 codons in all three frames in either orientation to prevent aberrant translational products. Six
171 independent transposon libraries were produced for each experimental condition using *S. pneumoniae*
172 strains TIGR4 or Taiwan-19F. Each transposon library consists of at least 10,000 total mutants. The
173 environmental conditions for selection experiments included growth in semi-defined minimal media
174 (SDMM) (van Opijnen & Camilli 2012) at pH 7.3 supplemented with 20 mM glucose, human alpha-1-
175 acid glycoprotein (Sigma – G9885), and agarose (Lonza – Seaplaque, 50101). Every selection
176 experiment was cultured at 37°C in a 5% CO₂ atmosphere.

177

178 **Microfluidic device production.**

179 Microfluidic device masks were designed using AutoCad 2016 software (AutoDesk) (Supplemental File
180 1) and photomasks were ordered from CAD/Art Services, Inc. (Bandon, OR). The mold and final
181 microfluidic chip fabrication was performed at the Integrated Sciences Cleanroom and Nanofabrication
182 Facility at Boston College. A master mold was fabricated by coating a silicon wafer with SU-8 3025

183 (MicroChem) using a spin coater (Laurell) and set by baking at 95°C. The photomask was aligned with
184 the silicon wafer and UV exposed followed by a post-exposure bake ramping from 65°C to 95°C over 4
185 minutes. The mold was developed using SU-8 developer (MicroChem) per the manufacturers guidelines
186 and rinsed with isopropanol and dH₂O followed by a hardening bake from 100C to 200C over 5 minutes.
187 The PDMS chip was generated by mixing PDMS and curing agent (Dow Corning, Sylgard 184) in a
188 10:1 ratio and added to the mold, degassed with a vacuum, and polymerized at 65°C overnight.
189 Polymerized PDMS was cut from the mold and a biopsy punch (0.75mm – Shoney Scientific) was used
190 to create ports for tubing (PE-2 tubing – Intramedic). PDMS slabs were bonded to glass (Corning – 2947,
191 75x50mm) at the clean room by washing the glass with acetone and isopropanol in a sonicator bath
192 while the PDMS was washed with isopropanol, followed by thorough drying with filtered nitrogen gas.
193 The channel side of the PDMS slab and the glass slide were treated with plasma (400sccm flow; 400
194 watts; 45 sec) using a faraday barrel screen. Plasma treated surfaces were quickly brought into contact
195 and pressed together and then placed at 65°C for 10 minutes to complete bonding.

196

197 **Droplet production and culturing of bacteria in liquid and agarose droplets.**

198 Before droplet production the device's aqueous channel was primed with Aquapel (Aquapel #47100)
199 and then flushed with fluorinated oil (Novec 7500 oil; 3M #98-0212-2928-5) (Fig. 1b). Devices were
200 used immediately or incubated overnight at 65°C, covered in scotch tape, and then stored in the dark for
201 several weeks before use. A 1ml syringe (BD – 309628) was filled with 1.5% of PicoSurf-1 in Novec
202 7500 oil (Dolomite; 3200214) while another 1ml syringe was filled with cell culture and then both were
203 hooked into syringe pumps (Cole-Parmer Instrument Co. – 00280QP). PE-2 tubing was used to transfer
204 PicoSurf-1 oil to the 'oil inlet', cell culture to the 'aqueous inlet', and collect droplets from the 'droplet
205 outlet' (Fig. 1b). Cells were diluted based on droplet size and according to a Poisson distribution with
206 the goal of generating droplets that contained a single bacterial cell (Shapiro 2003). With our device a
207 concentration of 2.1×10^6 cells/ml encapsulated into ~157pL sized droplets will yield approximately 74%
208 empty droplets, 22% with single cells, and 3% with two or more cells. The syringe pump rate for cell
209 encapsulation was 400 $\mu\text{l hr}^{-1}$ yielding $\sim 1.4 \times 10^6$ total droplets in 30 minutes. To generate agarose
210 droplets the entire droplet production system was placed in a 37°C warm room. 1% Seaplaque agarose
211 was added to growth media and then heated until dissolved. The agarose was then filtered (0.22 μm) after
212 which the cells were added to the agarose solution. After production, agarose droplets were gelled at 4°C
213 for 10 min with occasional shaking, and then transferred to the incubation chamber. To produce growth
214 curves small fractions of droplet culture were collected and broken open with 1H,1H,2H,2H-perfluoro-
215 1-octanol (PFO; Sigma-Aldrich – 370533), which separated oil and aqueous culture phases. For liquid

216 droplets the aqueous culture phase was immediately plated for live cell counts while the aqueous phase
217 for agarose droplets was added to a dounce homogenizer to break up the agarose to release cells for live
218 cell plating. CFU-fold expansion was calculated by dividing CFU counts at every time point by the
219 initial CFU count at the beginning of each experiment. A *student's t-test* was used to determine if
220 expansion between samples was significantly different (* $p < 0.05$, ** $p < 0.005$, *** $p < 0.0005$).

221

222 **DNA sample preparation, Illumina sequencing, and fitness calculation.**

223 Genomic DNA (gDNA) was extracted using the DNeasy Blood & Tissue Kit according to the
224 manufacturer's guidelines for Gram-positive bacteria (Qiagen – 69506). DNA adapter barcodes were
225 made by mixing an equal volume of primers ADBC-F and ADBC-R (Supplementary Table 6) at a
226 concentration of 0.2 nM in buffer (10mM Tris-base, 50mM NaCl, 1mM EDTA, pH 8), followed by
227 incubation at 95°C for 3 min, 60°C 10 min, 55°C 10 min, 50°C 20 min, 45°C 30 min, 42.5°C 15 min,
228 40°C 15 min, 21°C 1 min, and held at 4°C. Illumina DNA sample preparation for Tn-Seq was performed
229 depending on the amount of gDNA collected. High gDNA amounts (>500ng) were prepared with a
230 standard Illumina preparation method for Tn-Seq as previously described (van Opijnen & Camilli 2010).
231 Low gDNA input amounts (<500ng) were prepared by first performing whole-genome amplification
232 (WGA) on the gDNA sample using phi29 DNA polymerase (NEB - M0269S). 10ng of gDNA was
233 mixed with 10µM exo-resistant primer (MCLAB – ERRP-100), 2.5mM dNTP, and 1X phi29 DNA
234 polymerase reaction buffer, in a total volume of 26.25µl, and incubated at 95°C for 3 min and then
235 placed on ice. Next 1XBSA (NEB), and 2 units of phi29 (0.57U/ml), were added to the reaction, and
236 incubated for 7 hrs at 30°C, 10 min at 65°C, and held at 4°C. 10µl magnetic beads (Axygen – AxyPrep
237 Mag PCR Clean-up Kit, MAGPCRCL50) were mixed with 30µl of freshly made PEG solution (20%
238 PEG8000, 2.5M NaCl, 10mM Tris-base, 1mM EDTA, 0.05% tween20, pH8) and added to the 30µl
239 sample, mixed, and incubated at room temperature for 20 min. A magnet was used to separate the
240 bead/DNA complex from the PEG solution and the beads were washed 3 times in 200µl 70% ethanol
241 (all magnetic bead washes were performed this way). Beads were then dried for 3 minutes at room
242 temperature, and DNA was eluted off the beads with 12.7µl of dH₂O. 11.49µl of phi29 amplified DNA
243 was then added to a MmeI digestion mix (2 units NEB MmeI enzyme, 50µM SAM, 1X CutSmart Buffer)
244 in a total volume of 20µl, and incubated for 2.5 hrs at 37°C followed by 20 min at 65°C. 1µl of alkaline
245 phosphatase (NEB - M0290S Calf Intestinal, CIP) was added to the sample and incubated for 1 hr at
246 37°C. 10µl magnetic beads plus 20ul PEG solution per sample was used to wash the sample followed by
247 elution in 14.3µl of dH₂O. T4 DNA ligase (NEB M0202L) was used to ligate DNA adapter barcodes by
248 adding 13.12µl DNA to 1µl of 1:5 diluted adapter, 1X T4 DNA Ligase Reaction Buffer, and 400 units

249 T4 DNA ligase, followed by incubation at 16°C for 16 hrs, 65°C for 10 min and held at 10°C. 10µl
250 magnetic beads plus 20µl PEG solution was used to wash the sample followed by elution in 36µl of
251 dH₂O. Adapter ligated DNA was then PCR amplified using Q5 high-fidelity DNA polymerase (NEB –
252 M0491L) by adding 34µl of DNA to 1X Q5 reaction buffer, 10mM dNTPs, 0.45µM of each primer (P1-
253 M6-GAT-MmeI; P2-ADPT-Tnseq-primer; Supplementary Table 6), 1 unit Q5 DNA polymerase, and
254 incubated at 98°C for 30 sec, and 18-22 cycles of 98°C for 10 sec, 62°C for 30 sec, 72°C for 15 sec,
255 followed by 72°C for 2 min and a 10°C hold. PCR products were gel purified and sequenced on an
256 Illumina NextSeq 500 according to the manufacturers protocol. Sequence analysis was performed with a
257 series of in-house scripts as previously described (van Opijnen et al. 2009; McCoy et al. 2017). The
258 fitness of a single mutant (W_i) is calculated by comparing the fold expansion of the mutant to the fold
259 expansion of the population and is determined by the following equation (van Opijnen et al. 2009):

$$W_i = \frac{\ln(N_i(t_2) \times d / N_i(t_1))}{\ln((1 - N_i(t_2)) \times d / (1 - N_i(t_1)))}$$

260 in which $N_i(t_1)$ and $N_i(t_2)$ are the mutant frequency at the beginning and end of the experiment
261 respectively and d is the population expansion. The final average fitness and standard deviation are
262 calculated across all insertions within a gene, and since fitness is calculated using the expansion factor
263 of the population, W_i becomes independent of time, therefore allowing comparisons between different
264 strains and conditions across different experiments. To determine whether fitness effects are
265 significantly different between conditions three requirements had to be fulfilled: 1) W_i is calculated from
266 at least three data points, 2) the difference in fitness between conditions has to be larger than 10% (thus
267 $W_i - W_j = < -0.10$ or > 0.10), and 3) the difference in fitness has to be significantly different in a one
268 sample t -test with Bonferroni correction for multiple testing (van Opijnen et al., 2009, 2016, van
269 Opijnen and Camilli 2012, 2013).

270

271 **Mutant generation.**

272 Gene knockouts were constructed by replacing the entire coding sequence with a chloramphenicol or
273 spectinomycin resistance cassette through overlap extension PCR. Construction of PCR products for
274 gene replacement and transformation of *S. pneumoniae* were performed as described previously (van
275 Opijnen & Camilli 2010; Iyer et al. 2005). Generated mutant strains and primers for marked deletions
276 can be found in Supplemental Information (Supplementary Table 6,7).

277

278 **Co-culture assays.**

279 To validate genetic phenotypes associated with carbon utilization from AGP, single-gene mutants (mt)
280 were co-cultured with their wildtype parental strain (wt) in a 1:20 ratio (mt:wt). Mutant and WT
281 frequencies were calculated by live cell plating on blood agar plates with or without antibiotics. Fitness
282 of the mutant was then calculated as described as previously and above (van Opijnen et al. 2009).

283

284 **Visualization of cells and droplets.**

285 Images of cells and droplets were captured with an Olympus IX83 inverted microscope. For planktonic
286 batch culture 10 μ l of cells were stained with 0.5 μ l green-fluorescent SYTO-9 (1:10 dilution in PBS) and
287 0.5 μ l red-fluorescent propidium iodide (1:10 dilution in PBS) (Thermo Fisher Scientific – L34856).
288 Batch culture cells were then mounted between an agar pad and coverslip for visualization. All droplet
289 images were produced by mounting samples between coverslip spacers to prevent droplets from being
290 compressed.

291

292 **Gene expression analysis.**

293 Immediately after culture the cells were pelleted and snap-frozen in an ethanol/dry-ice bath, followed by
294 RNA isolation using RNeasy Mini Kit (Qiagen – 74106) according to the manufacturer’s guidelines.
295 RNA was treated to remove genomic DNA with TURBO DNA-free kit (Invitrogen – AM1907). cDNA
296 was made from 400ng of DNA-free RNA using iScript Reverse Transcription Supermix (Bio-Rad –
297 1708841). Primers for quantitative real-time PCR (qRT-PCR) were designed using Primer3 software
298 (Untergasser et al. 2012; Koressaar & Remm 2007) (Supplementary Table 6). qRT-PCR was performed
299 with iTaq SYBR Green Supermix (Bio-Rad – 1725124) using 2 μ l of cDNA in a MyiQ Real-Time PCR
300 Detection System (Bio-Rad). Each sample was measured in technical and biological triplicates and
301 normalized to the 50S ribosomal protein SP_2204.

302

303 **Data availability.**

304 All sequence data can be found under the NCBI Sequence Read Archive accession SRP154922.

305

306 **Acknowledgements**

307 This work was supported by R01-AI110724 and U01-AI124302 to TvO.

308

309 **Author contributions**

310 TvO, DT and PJ conceived and worked out the idea. DW provided the initial microfluidics device and
311 mask. PJ, DT and SW designed, produced and characterized microfluidics devices. DT performed
312 experiments. DT and TvO performed data analyses. DT and TvO wrote the manuscript.

313

314 **Competing interests**

315 The authors declare no competing interests.

316

317 **Acknowledgments**

318 We would like to thank David A. Weitz and Lloyd Ung for providing, and assistance with, the initial
319 microfluidic device. Additionally, we would like to thank Stephen Shepard at the Integrated Sciences
320 Cleanroom at Boston College.

321

322 **Figure Legends**

323

324 **Figure 1 | Droplet Tn-Seq overview and characterization. (a)** A microfluidic device encapsulates
325 single bacterial cells into liquid-in-oil droplets. Bacteria are allowed to expand within droplets, gDNA is
326 isolated at the start of the experiment (t1) and after expansion (t2) and is amplified with phi29.
327 Importantly, while expansion for each transposon mutant takes place in isolation, gDNA is isolated from
328 the pooled population, enabling screening of all mutants simultaneously. gDNA is digested with MmeI,
329 an adapter is ligated, a ~180bp fragment is produced which contains approximately 16 nucleotides of
330 bacterial genomic DNA, defining the transposon insertion location, followed by Illumina sequencing.
331 Reads are demultiplexed (based on the barcode in the adapter and a potential second barcode in primer
332 1), mapped to the genome, and fitness is calculated for each defined region. **(b)** Syringe pumps and
333 tubing are used to deliver surfactant in a fluorinated carrier oil to the Oil-inlet (1) and culture media
334 containing cells to the Aqueous inlet (2). Resistors (3) reduce fluctuation in liquid flow rates. Oil
335 separates the continuous flow of the cell culture into monodisperse droplets at the Flow-focus junction
336 (4). Droplets exit the device through the Droplet-outlet (5) and are collected. **(c)** Depending on the size
337 of the channels, and oil and aqueous phase flow rates, uniformly sized droplets can be formed ensuring
338 each cell has the same expansion potential. With a channel size of 40 μM ~67 μM diameter droplets are
339 created. **(d)** Liquid droplets in carrier oil. Scale bar, 50 μM . **(e)** Both Gram-positive and negative bacteria
340 expand robustly in liquid droplets, in a similar fashion to batch culture (i.e. a 5ml culture). Depending on
341 the experiment the amount of gDNA may be limited, which can be resolved by whole genome
342 amplification (WGA), which introduces no bias compared to a standard Tn-Seq library prep **(f)** and is
343 reproducible **(g)**.

344

345 **Figure 2 | dTn-Seq validation. (a)** Wt has a shorter chain length than ΔlytB in batch culture, but in
346 droplets chain lengths are similar. **(b)** Wt and ΔlytB expand and grow at a similar rate in batch-culture,
347 however, in droplets ΔlytB expands less than wt. Shorter chain lengths and less expansion of ΔlytB in
348 droplets could either be caused by slower growth or a higher death rate. **(c)** Gene expression analyses
349 shows significant upregulation of competence genes *comD*, *E*, *M*, and *X*, with the autolysin *cbpD* being
350 upregulated ~28-fold in droplets, indicating that fratricide and thus an increased death rate is limiting
351 growth of ΔlytB in droplets. Moreover, this indicates a new role for LytB, which is to suppress local
352 hyper-competence. **(d)** While deletion mutants of SP_1415, SP_1674, SP_1685, and SP_2056 have no
353 defect when grown independently in medium with glucose as the carbon source (orange bars), they
354 hardly grow when glucose is replaced by AGP (green bars). Importantly, this growth defect in AGP can

355 be resolved by adding wt to the culture (blue bars), indicating that wt is providing ‘community support’.
356 (e) Agarose droplets can be generated by adding low melting agarose to growth media, which provides
357 structural support and results in bacteria (Gram-negative and positive alike) growing in microcolonies.
358 Scale bars 50µM. (f, g) Two capsule mutants (SPT_0394 and SPT_0395) that grow (very) slow in liquid
359 batch culture and liquid droplets, expand robustly in agarose droplets. *p<0.05, **p<0.005,
360 ***p<0.0005 in a *student t-test*.
361

Figure 1

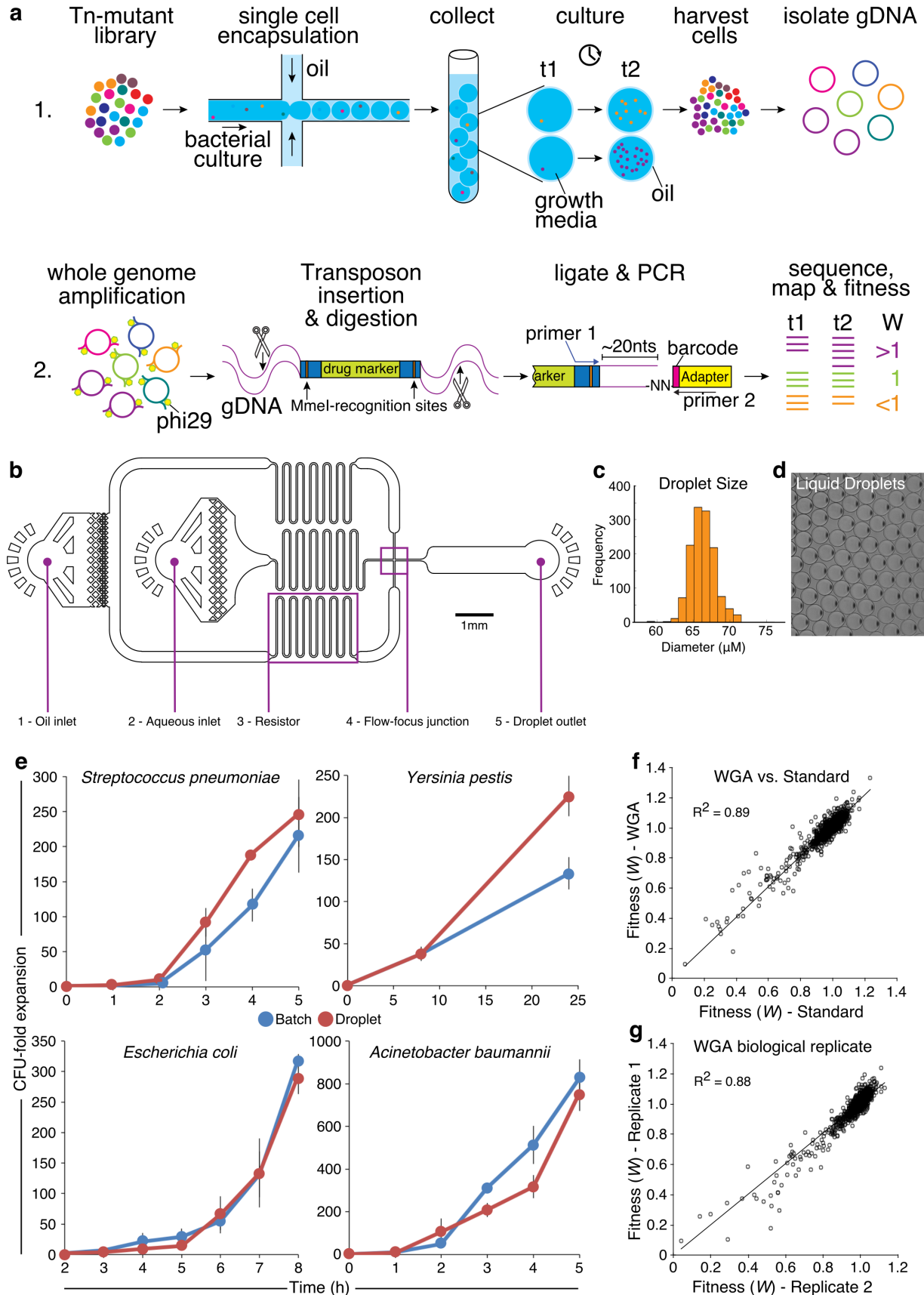
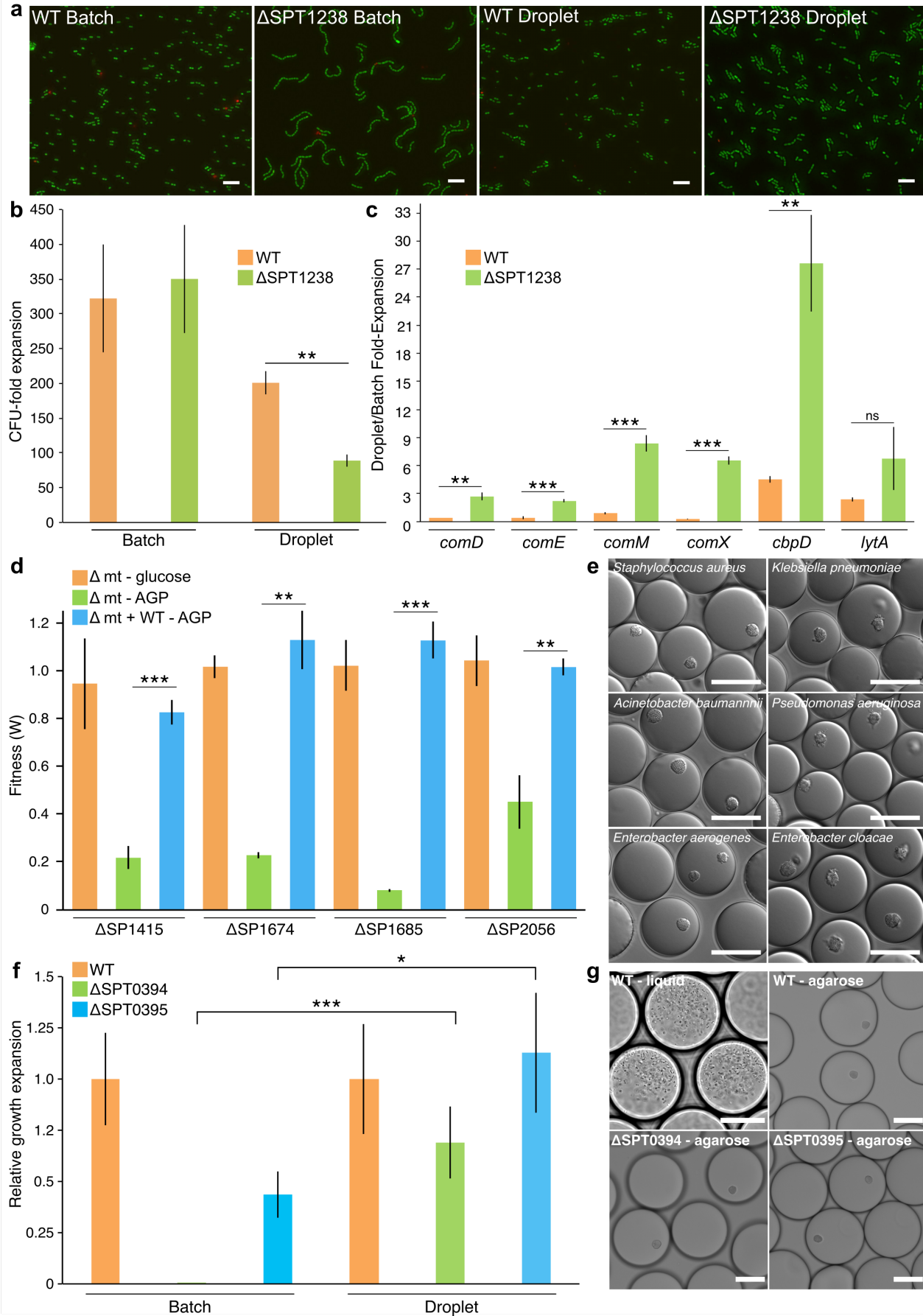


Figure 2



364 **References.**

365

366 Domenech, A., Slager, J. & Veening, J., 2018. Antibiotic-induced cell chaining triggers pneumococcal
367 competence by reshaping quorum sensing to autocrine signaling. *BioRxiv*, pp.1–9.

368 Domenech, M., García, E. & Moscoso, M., 2012. Biofilm formation in *Streptococcus pneumoniae*.
369 *Microbial Biotechnology*, 5(4), pp.455–465.

370 García, P. et al., 1999. LytB, a novel pneumococcal murein hydrolase essential for cell separation.
371 *Molecular Microbiology*, 31(4), pp.1275–1281.

372 Iyer, R., Baliga, N.S. & Camilli, A., 2005. Catabolite Control Protein A (CcpA) Contributes to
373 Virulence and Regulation of Sugar Metabolism in *Streptococcus pneumoniae*. *Journal of*
374 *Bacteriology*, 187(24), pp.8340–8349.

375 King, S.J., 2010. Pneumococcal modification of host sugars: A major contributor to colonization of the
376 human airway? *Molecular Oral Microbiology*, 25(1), pp.15–24.

377 Koressaar, T. & Remm, M., 2007. Enhancements and modifications of primer design program Primer3.
378 *Bioinformatics*, 23(10), pp.1289–1291.

379 Lam, J. et al., 1980. Production of mucoid microcolonies by *Pseudomonas aeruginosa* within infected
380 lungs in cystic fibrosis. *Infection and Immunity*, 28(2), pp.546–556.

381 McCoy, K.M., Antonio, M.L. & van Opijnen, T., 2017. MAGenTA: a Galaxy implemented tool for
382 complete Tn-Seq analysis and data visualization. *Bioinformatics (Oxford, England)*, 33(17),
383 pp.2781–2783.

384 Moye, Z.D., Burne, R.A. & Zeng, L., 2014. Uptake and metabolism of N-acetylglucosamine and
385 glucosamine by *Streptococcus mutans*. *Applied and Environmental Microbiology*, 80(16), pp.5053–
386 5067.

387 van Opijnen, T., Bodi, K.L. & Camilli, A., 2009. Tn-seq: high-throughput parallel sequencing for fitness
388 and genetic interaction studies in microorganisms. *Nature methods*, 6(10), pp.767–72.

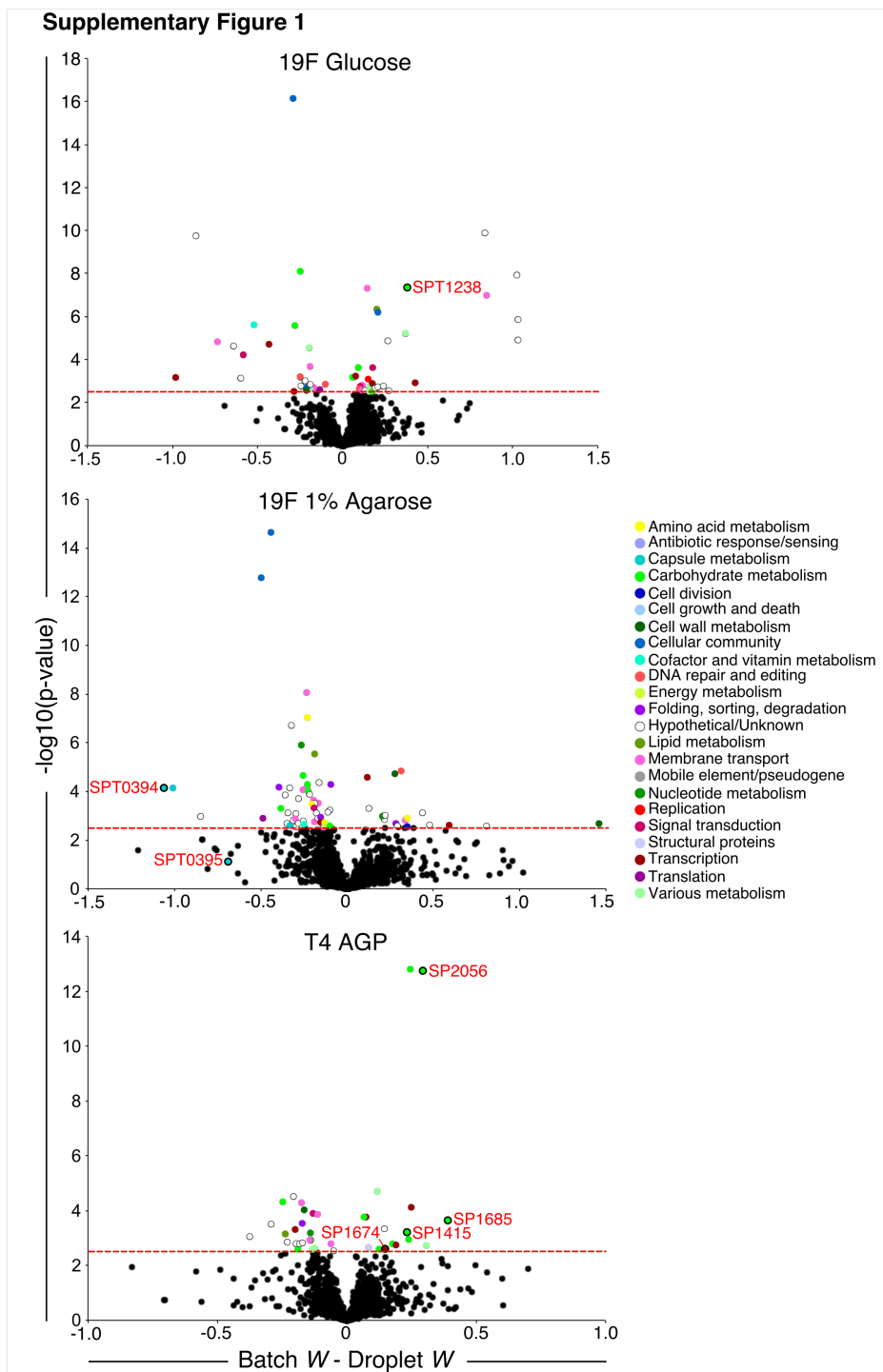
389 van Opijnen, T. & Camilli, A., 2012. A fine scale phenotype-genotype virulence map of a bacterial
390 pathogen. *Genome research*, 22(12), pp.2541–51.

391 van Opijnen, T. & Camilli, A., 2013. Transposon insertion sequencing: a new tool for systems-level
392 analysis of microorganisms. *Nature reviews. Microbiology*, 11(7), pp.435–42.

393 van Opijnen, T. & Camilli, A., 2015. Genome-wide fitness and genetic interactions determined by Tn-
394 seq, a high-throughput massively parallel sequencing method for microorganisms. *Current*
395 *protocols in microbiology*; 36: 1E.3.1–1E.3.24.

396 Pélissier, M.C. et al., 2014. Structural and functional characterization of the *Clostridium perfringens* N-

- 397 acetylmannosamine-6-phosphate 2-epimerase essential for the sialic acid salvage pathway. *Journal*
398 *of Biological Chemistry*, 289(51), pp.35215–35224.
- 399 Sæther, B. & Engen, S., 2015. The concept of fitness in fluctuating environments. *Trends in ecology &*
400 *evolution*, 30(5), pp.273–281.
- 401 Shapiro, H.M., 2003. Practical Flow Cytometry. *Wiley-Liss*, 4th edn.
- 402 Sriramulu, D.D. et al., 2005. Microcolony formation: A novel biofilm model of *Pseudomonas*
403 *aeruginosa* for the cystic fibrosis lung. *Journal of Medical Microbiology*, 54(7), pp.667–676.
- 404 Untergasser, A. et al., 2012. Primer3-new capabilities and interfaces. *Nucleic Acids Research*, 40(15),
405 pp.1–12.
- 406 Veening, J.-W., Smits, W.K. & Kuipers, O.P., 2008. Bistability, Epigenetics, and Bet-Hedging in
407 Bacteria. *Annual Review of Microbiology*, 62(1), pp.193–210.
- 408 Worlitzsch, D. et al., 2002. Effects of reduced mucus oxygen concentration in airway *Pseudomonas*
409 infections of cystic fibrosis patients. *The Journal of Clinical Investigation*, 109(3), pp.317–325.
- 410
- 411
- 412
- 413
- 414



415

416 **Supplementary Figure 1** | Approximately 2-5% of genes confer a significantly different fitness in
417 droplets compared to batch culture. The functions of these significant genes span a wide range of
418 categories including metabolism, transport, regulation and cell wall integrity. The red-dashed line
419 indicates a conservative threshold for significance ($-\log(p\text{-value}) > 2.5$; $p\text{-value} < 0.003$). All genes above
420 the line are labeled with a color corresponding to a functional category represented in the figure key.
421 The 7 genes that were validated in the study are outlined in black circles and marked with gene numbers.

422

423

424

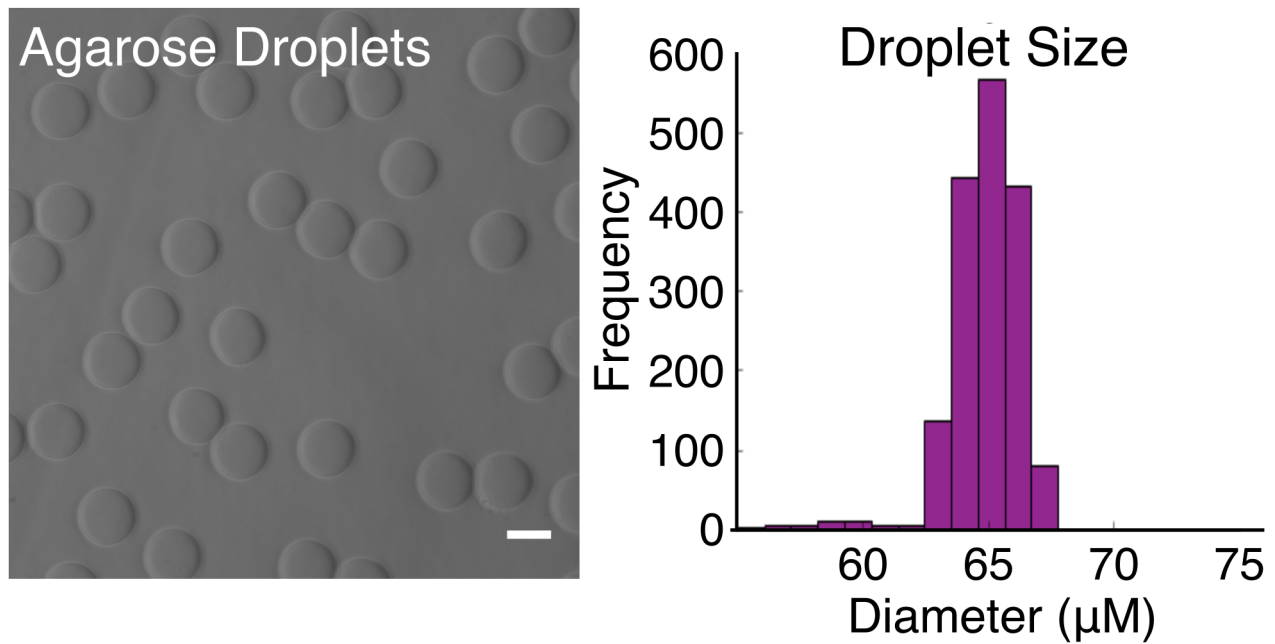
425

426

427

428

Supplementary Figure 2



429

430

431 **Supplementary Figure 2** | Agarose droplets with carrier oil removed. The 40μM device makes

432 monodisperse agarose droplets that are ~65μM in diameter (~144pL volume). Scale bar is 50μM.

433